

~~CONFIDENTIAL~~

281

Copy
RM L52K10

NACA RM L52K10

0144427

TECH LIBRARY KEEPS NACA



RESEARCH MEMORANDUM

S83L

PRELIMINARY INVESTIGATION OF THE TOTAL-PRESSURE-RECOVERY
CHARACTERISTICS OF A 15° SEMIANGLE MOVABLE-CONE
VARIABLE-GEOMETRY RAM-JET INLET AT FREE-JET
MACH NUMBERS OF 1.62, 2.00, 2.53, AND 3.05

By Arthur H. Hinners, Jr., and John B. Lee

Langley Aeronautical Laboratory
Langley Field, Va.

~~RECEIPT OF SIGNATURE
IS REQUIRED~~

CLASSIFIED DOCUMENT

This material contains information affecting the National Defense of the United States within the meaning of the espionage laws, Title 18, U.S.C., Secs. 793 and 794, the transmission or revelation of which in any manner to an unauthorized person is prohibited by law.

NATIONAL ADVISORY COMMITTEE
FOR AERONAUTICS

WASHINGTON

January 8, 1953

~~CONFIDENTIAL~~

NATIONAL ADVISORY COMMITTEE FOR AERONAUTICS

RESEARCH MEMORANDUM

PRELIMINARY INVESTIGATION OF THE TOTAL-PRESSURE-RECOVERY

CHARACTERISTICS OF A 15° SEMIANGLE MOVABLE-CONE

VARIABLE-GEOMETRY RAM-JET INLET AT FREE-JET

MACH NUMBERS OF 1.62, 2.00, 2.53, AND 3.05

By Arthur H. Hinners, Jr., and John B. Lee

SUMMARY

A preliminary investigation of a 15° semiangle movable-cone variable-geometry ram-jet inlet was conducted in the preflight jet to determine the variable-geometry effect on total-pressure recovery at free-jet Mach numbers of 1.62, 2.00, 2.53, and 3.05, at zero angles of attack and yaw.

Maximum total-pressure-recovery values attained were 0.90, 0.82, 0.61, and 0.43 at free-jet Mach numbers of 1.62, 2.00, 2.53, and 3.05, respectively. All values of maximum total-pressure recovery occurred at a diffuser exit Mach number of 0.25. The maximum total-pressure limit was reached at the beginning of "buzz" caused by separation of the flow off the cone surface.

In general, increasing the cowling-position parameter increased the value of both total-pressure recovery and mass-flow ratio.

A benefit in increased total-pressure recovery and mass-flow ratio was found for the movable-cone variable-geometry inlet over a fixed-area inlet that would be able to operate below the buzz limit.

INTRODUCTION

In the design of a fixed-area ram-jet inlet the inlet area ratio and the oblique shock configuration are selected to provide the desired mass flow, total-pressure recovery, and external drag at the design Mach number of the inlet. At lower than the inlet design Mach numbers, the air mass-flow requirements of the burner are less, but the inlet cannot efficiently reduce the air mass flow into the inlet. Generally,

the contraction ratio of the inlet or the back pressure forces a normal shock in front of the inlet cowl. The resulting external drag has been found to increase greatly over the external drag of an inlet designed to operate at these lower Mach numbers. This poor matching of the inlet and burner at below-design Mach numbers generally results in lower total-pressure recovery and thrust production. It therefore becomes evident that a variable-geometry inlet, which can efficiently match the air-flow requirements of the burner to the inlet over a range of Mach numbers, is needed.

The variable-geometry inlet discussed in this paper consists of a cone which can be moved axially with respect to the inlet cowl so as to provide supercritical flow over a range of Mach number. At below-design Mach numbers, by extending the cone forward of design condition, the conical shock is placed farther away from the cowl lip and thus reduces the air mass flow entering the inlet. As the Mach number is increased the cone can be retracted to increase the air mass flow. For a cowling-position parameter of 25.0° , the conical shock of the movable cone would intersect the cowl lip at a Mach number of 3.05. This Mach number for a fixed-area inlet is commonly called the design Mach number.

Studies of supercritical additive drag show that reducing the cone angle reduces the additive drag. Tests made of fixed-area conical inlets (ref. 1) have shown that decreasing the cone angle tends to decrease the obtainable pressure recovery. A 15° semiangle cone was chosen to try to obtain a reasonable compromise between external drag and total-pressure recovery in order to obtain a net propulsive force over a range of Mach number.

This preliminary report concerns the variable-geometry effect on total-pressure recovery. The investigation was conducted in the preflight jet of the Pilotless Aircraft Research Station at Wallops Island, Va., with a ram-jet model having a diameter of 6.60 inches and a length of 50.77 inches.

The data presented were obtained with cold flow at free-jet Mach numbers of 1.62, 2.00, 2.53, and 3.05 at 0° angles of attack and yaw. The Reynolds number range of these tests is shown in table I.

SYMBOLS

d diameter, in.
H total pressure, lb/sq ft
m measured mass flow through duct, slugs/sec

m_0	mass flow through a stream tube of area equal to inlet capture area under free-stream conditions, slugs/sec
M	Mach number
M_l	Mach number at inlet lip of cowl
P	static pressure, lb/sq ft
r	radius of duct at measuring station, in.
R_e	Reynolds number, based on inlet cowl diameter of lip
R	gas constant, 53.3 ft/ $^{\circ}$ R
S	cross-sectional area of duct, sq ft
S_c	inlet capture area defined by cowl lip; 0.164 sq ft
S_e	entrance area to diffuser defined along imaginary surface perpendicular to cone surface from leading edge of inlet, sq ft
T	static temperature, $^{\circ}$ R
V	velocity, ft/sec
x	distance from cowl leading edge (positive downstream), in.
y	ordinate or location of total-pressure tube measured from center, in.
ρ	density, slugs/cu ft
θ_l	cowling-position parameter (angle between axis of diffuser and line joining apex of cone to lip of cowl)

Subscripts:

0	free stream
1	a point station behind the conical shock
2	cone surface
3	station of minimum internal area or diffuser throat
4	diffuser exit and combustion-chamber entrance station

5 combustion-chamber exit station
6 exit choking station ($M_6 = 1.00$)
d local point station

MODEL

Two photographs of the ram-jet inlet model and a sketch of the model tested are presented as figures 1 and 2, respectively. The overall length of the inlet and simulated combustion chamber is 50.77 inches, with a maximum external diameter of 6.60 inches. This configuration size, weight, and potential thrust output is sufficient for two of these ram-jet engines to propel a missile test vehicle approximately 16 feet long and 250 pounds total weight.

The conical inlet had an inlet cowl that was 5.48 inches in diameter at the lip, and varied to a maximum outside diameter of 6.60 inches and an inside diameter of 6.00 inches. Coordinates of the inlet cowl are given in table II. The cowl had internal and external lip angles of 6° and 13° , respectively.

The movable 15° semiangle cone had a maximum diameter of 4.46 inches. This cone could be moved axially during the tests by means of a hydraulic piston located within the central body. At the innermost position, the cone tip projected 5.83 inches in front of the cowl lip and could be moved axially a total of 2.88 inches forward from this point. Coordinates of this movable cone are given in table II. The ratio of the central-body maximum diameter to the cowl-lip diameter is 0.814.

Rearward of the innermost position of the cone, the central body was supported by three equally spaced circular-arc support struts and had a conical variation to the burner attachment point at the downstream end of the central body. An idea of the rate of subsonic diffusion can be obtained from the variation of geometric-area ratio from the leading edge of the inner-body support struts to the diffuser-exit-rake station, as presented in figure 3. The variation of internal-contraction ratio as a function of the cowling-position parameter θ_l is presented in figure 4.

At the end of the subsonic diffuser, the diameter increased to the maximum internal diameter of 6.50 inches. The outlet area for each test was fixed by a plug. The plug was centered in the exit of the simulated combustion chamber by a rod supported by three circular-arc support struts. Appropriate plug diameters were selected to give a variation in diffuser exit Mach number M_4 of 0.20 to 0.27.

The station notation used in data presentation and analysis is shown in figure 5.

Tests and Methods

The tests were made in the preflight jet of the Pilotless Aircraft Research Station at Wallops Island, Va. (ref. 2). Nozzles which were 12 by 12 inches square were used for jet test Mach numbers of 1.62 and 2.00. Round nozzles of 8- and $\frac{7}{2}$ -inch diameters were used for jet Mach numbers of 2.53 and 3.05, respectively.

The model was placed in the exit of the jet nozzle so that the inlet would be within the Mach diamond of the nozzle. In most tests the movable cone was extended at the start of the test and moved axially into the model until a condition of unsteady flow called "buzz" began, at which time the direction of travel was reversed. At least one cycle of movement of the cone was made for each test. The model throughout all tests was at 0° angles of attack and yaw. The variation of Reynolds number based upon cowl entrance diameter of 5.84 inches is presented in table I.

The average total pressure at the diffuser exit station H_4 was determined by integration of the measured profiles as follows:

$$H_4 = \int_0^1 H_d d\left(\frac{y}{r}\right)^2$$

The mass-flow ratio m/m_0 was obtained by use of the following expression:

$$\frac{m}{m_0} = \frac{p_6^{S_6} V_6}{p_0^{S_c} V_0} = \frac{\frac{p_6^{S_6} M_6}{\sqrt{T_6}}}{\frac{p_0^{S_c} M_0}{\sqrt{T_0}}}$$

By substituting the pressure and temperature ratios for $M = 1$ at station 6 and the pressure and temperature ratios for each free-jet Mach number at station 0, the expression can be reduced to

$$\frac{m}{m_0} = K \frac{H_6}{H_0} \frac{S_6}{S_c}$$

where

$$K = \frac{1}{M_0} \left(\frac{1 + \frac{\gamma - 1}{2} M_0^2}{\frac{\gamma - 1}{2}} \right)^{\frac{\gamma+1}{2(\gamma-1)}}$$

The total-pressure recovery H_5/H_0 was determined at station 5 and negligible losses were assumed between stations 5 and 6.

Results from tests made using the same simulated combustion chamber and exit-station rakes on a similar central-body inlet in which the full known capture area could be obtained indicated that a mass-flow correction factor was not required for this instrumentation. Integration of the mass flow across radial stations at the diffuser exit station indicated the same conclusion.

Instrumentation

Total pressure at the diffuser exit station was determined by nine total-pressure tubes arranged in two rakes, centrally located between the inner-body support struts. One rake had a static probe located at the center of the rake and wall static pressures were measured near each rake.

Average total pressure at the combustion-chamber exit station was obtained using three equally spaced rakes, each having six tubes spaced at radial stations of equal area. The tubes of each rake were connected to a common pressure chamber within the rake. The measured chamber pressures of the three rakes were arithmetically averaged to obtain average total pressure at this station.

Other measurements made were the free-stream total pressure in the chamber just before the free-jet supersonic nozzle and the stream static

pressure at the exit of the free-jet nozzle. The position of the movable cone was measured by a linear control-position indicator. Pressures were recorded by mechanical optical pressure recorders and electrical pressure recorders of the strain-gage type. Time histories were obtained on film and paper records which were time-correlated with a 10-cycle-per-second timer. Shadowgraphs were obtained by using a carbon-arc light source and an opaque-glass screen.

Accuracy

Instruments used in these tests were accurate to 1 percent of their full-scale range. By accounting for this error and also by observing the scatter of points in repeated tests, the magnitude of the maximum possible error is believed to be within the following limits:

M_0 (1.62 and 2.00)	±0.01
M_0 (2.53 and 3.05)	±0.02
M_4	±0.003
H_4/H_0	±0.02
m/m_0	±0.02
θ_l	±0.10°

RESULTS AND DISCUSSION

The total-pressure recovery H_4/H_0 of the variable-geometry inlet is presented as a function of the cowling-position parameter θ_l in figure 6. The theoretical values of the maximum total-pressure recovery H_4/H_0 with cowling-position parameter were calculated as in reference 2 by assuming the average entrance Mach number to be $\frac{M_l + M_2}{2}$ and by neglecting subsonic diffuser losses as well as the effects of the internal oblique shock originating at the lip of the cowl. The values of M_l and M_2 , as well as the total-pressure loss through the conical shock, were found by the table of reference 3. Theoretical starting positions are found to be $\theta_l = 19.56^\circ$ and 21.35° for free-stream Mach numbers of 1.62 and 2.00, respectively. At values of θ_l less than the value of the starting position, the normal shock could enter the inlet at the test Mach number, whereas at greater values of θ_l , the shock could not enter the inlet. If the diffuser was started at the test Mach number of 1.62, theoretically the shock could remain within the diffuser for values of θ_l up to 20.26° , at which point a Mach number of 1 is reached at the minimum. For the test Mach number of 2.00, the started condition theoretically could exist for all values

of θ_l of these tests. Two possible theoretical total-pressure recoveries were then considered; the case of the normal shock at the entrance lip, and the case of the shock at the diffuser throat or minimum station. The theoretical total-pressure recovery is higher when the normal shock is located at the diffuser throat because of the reduction in the internal stream Mach number in the converging area to the throat. For free-stream Mach numbers of 2.53 and 3.05, the inlet is started for the full range of θ_l tested.

The data points of total-pressure recovery as a function of θ_l are presented for diffuser-exit Mach numbers M_4 of 0.20, 0.22, 0.25, and 0.27. A choking plug as shown in figure 2 was used in each test, fixing the diffuser exit Mach number to the values presented. For each value of M_4 , as θ_l increased, H_4/H_0 increased until, in all cases except $M_4 = 0.27$, a condition of unsteady flow was reached which has been called buzz. This condition of buzz was in these tests the upper limit of obtainable total-pressure recovery. At $M_4 = 0.27$ it was not mechanically possible in these tests to move the cone into the cowl beyond a value of $\theta_l = 25.0^\circ$, and the buzz limit was not reached.

For a given value of θ_l , with supercritical flow in the inlet, increasing M_4 (that is, increasing the exit area) relocates the normal shock in the divergent portion of the diffuser with an increase in Mach number before the normal shock occurs; this increase causes a stronger normal shock and decreases the value of H_4/H_0 .

Then, if θ_l is increased, more mass flow enters the inlet and the total-pressure recovery must increase by the normal shock moving upstream toward the minimum area, until it is forced past the throat out in front of the entrance. Finally, a condition is reached when buzz begins. Increasing M_4 locates the normal shock farther downstream inside the inlet; this location allows larger values of θ_l , and therefore, higher values of H_4/H_0 to be reached before buzz occurs.

Total-pressure recovery for corresponding mass-flow ratios m/m_0 is presented in figure 7 for the four test Mach numbers. In all cases, increasing m/m_0 by moving the cone into the inlet increased the total-pressure recovery. For the range of movement of the cone in these tests, values of m/m_0 of about 0.30 to 0.60 were obtained at $M_0 = 1.62$; 0.32 to 0.67 at $M_0 = 2.00$; 0.42 to 0.83 at $M_0 = 2.53$; and 0.61 to 0.96 at $M_0 = 3.05$. The dashed line indicates where buzz limits the maximum mass flow obtainable. The decrease in slope of this limit line at the higher values of m/m_0 indicates that the maximum value of H_4/H_0 that could be obtained with the 15° semiangle cone was closely approached in these tests.

Typical shadowgraphs of flow patterns are presented in figure 8. The shadowgraphs were photographed on the screen shown in figure 1 at an exposure of approximately 0.003 second. The shadowgraph pattern at $M_0 = 1.62, 2.00, 2.53$, and 3.05 indicates that a separation shock appears on the cone surface and tends to trigger the beginning of buzz. At $M_0 = 1.62$, evidence that the normal shock inside the inlet has moved to the inlet lip can be seen at a value of $\theta_l = 19.57$, with $M_4 = 0.25$. This value of θ_l was also verified at $M_4 = 0.27$ in shadowgraph patterns not presented. This value of θ_l is nearly the same value as the one-dimensional theoretical Mach number at which the inlet can start. It can be seen that a limited amount of subcritical operation was possible before buzz occurred.

At a Mach number of 2.00 the flow patterns indicate that the inlet could retain the normal shock until a value of $\theta_l = 22.35^\circ$ was reached, after being started at a lower value of θ_l . At $\theta_l = 22.35^\circ$, the separation shock can again be seen on the cone surface. Buzz occurs with apparently no possible subcritical operation.

The maximum total-pressure recovery attained for the four test Mach numbers is shown in figure 9 as a function of diffuser exit Mach number. At all Mach numbers tested, the maximum total-pressure recovery occurred at a diffuser exit Mach number of 0.25. Maximum total-pressure recovery values of 0.90, 0.82, 0.61, and 0.41 were attained at free-jet Mach numbers of 1.62, 2.00, 2.53, and 3.05, respectively. The value of maximum total-pressure recovery was reached at the onset of buzz at all diffuser exit Mach numbers except 0.27 where the buzz limit was not reached.

These maximum values of total-pressure recovery are presented as a function of free-stream Mach number in figure 10. A test point at a Mach number of 1.85 of a 15° semiangle cone, with a ratio of central-body diameter to cowl-lip diameter of 0.467 shows a value of $\frac{H_4}{H_0} = 0.87$ (ref. 4). At this same Mach number, the variable-geometry inlet of these tests with a ratio of central-body diameter to cowl-lip diameter of 0.814 and 6° to 13° cowl indicates a value of $\frac{H_4}{H_0} = 0.86$.

A 20° semiangle cone with a 7° to 10° cowl and a ratio of central-body diameter to cowl-lip diameter of 0.817 indicates that, at a Mach number of 2.75, a value of $\frac{H_4}{H_0} = 0.65$ (ref. 1) can be obtained while a value of $\frac{H_4}{H_0} = 0.54$ was obtained with the 15° semiangle cone of this test.

Total-pressure recovery as a function of free-stream Mach number is presented with lines of constant θ_l in figure 11 and with lines of corresponding constant mass-flow ratio in figure 12. These figures show the movable-cone variable-geometry effect on total-pressure recovery over the test range of Mach numbers and allow comparisons with the total-pressure recoveries of a fixed-area inlet, inasmuch as each value of constant θ_l represents a fixed-area inlet. The one-dimensional theoretical starting line where the normal shock could enter a fixed-area inlet is shown in figure 11. Values of θ_l above this starting line would prevent starting; below this line supercritical flow could be attained at the inlet.

By using the results shown in figure 11(b), with a diffuser exit Mach number of 0.25, a fixed-area inlet of design Mach number 3.05 and $\theta_l = 25.0^\circ$ would buzz over the entire range of test Mach number. In order to avoid buzz, this type of inlet would have to operate at a higher value of diffuser-exit Mach number. This figure indicates that a value of $\theta_l = 21.75^\circ$ or less would be required for a fixed-area inlet to operate buzz-free over this range of Mach number. The starting line indicates that this inlet would start at a value of $M_0 \approx 2.1$ and, at a Mach number of 3.05, would have a total-pressure recovery of 0.36.

In the case of the movable-cone variable-geometry inlet, the value of θ_l could be increased up to a value near the buzz limit starting at a Mach number of approximately 2.2, and higher values of total-pressure recovery could be attained through the remainder of the Mach number range than were possible with the fixed-area inlet. At a Mach number of 3.05, a value of $\theta_l = 24.0^\circ$ could be reached with a total-pressure recovery of 0.42. This represents an increase of about 16 percent in total-pressure recovery at this Mach number. Correspondingly, figure 12(b) shows that the fixed-area inlet of $\theta_l = 21.75^\circ$ would operate at a mass-flow ratio of 0.77 at $M_0 = 3.05$, while the variable-geometry inlet would be operating at a mass-flow ratio of 0.91, an increase of approximately 15 percent. This higher mass-flow ratio would be a benefit in a lower value of additive drag, as well as in increased value of thrust.

SUMMARY OF RESULTS

The following results were obtained from the tests of a 15° semi-angle movable-cone variable-geometry inlet at Mach numbers of 1.62, 2.00, 2.53, and 3.05:

1. Increasing the diffuser-exit Mach number by reducing the back pressure allowed the cone to be moved to a greater value of cowling-position parameter and resulted in higher values of total-pressure

recovery and mass-flow ratio. The maximum value of total-pressure recovery was attained at the highest mass-flow ratios and was limited by the start of buzz.

2. Maximum total-pressure-recovery values attained were 0.90, 0.82, 0.61, and 0.43 for free-jet Mach numbers of 1.62, 2.00, 2.53, and 3.05, respectively, with a diffuser-exit Mach number of 0.25.

3. A lower value of the cowling-position parameter than could be used at the design Mach number was required at below-design Mach numbers to avoid the occurrence of buzz. For this reason, the movable-cone variable-geometry inlet attained higher total-pressure recovery and mass-flow ratios over a range of Mach number from approximately 2.20 to the design Mach number of 3.05 than a corresponding fixed-area inlet that must operate below the buzz limit.

4. At the design Mach number of 3.05 the movable-cone diffuser realized a 16-percent increase in total-pressure recovery and a 15-percent increase in mass-flow ratio over the corresponding fixed-area inlet. This increase in total-pressure recovery and mass-flow ratio would result in an increased value of thrust and a lower value of additive drag.

Langley Aeronautical Laboratory,
National Advisory Committee for Aeronautics,
Langley Field, Va.

REFERENCES

1. Ferri, Antonio, and Nucci, Louis M.: Theoretical and Experimental Analysis of Low Drag Supersonic Inlets Having a Circular Cross Section and a Central Body at Mach Numbers of 3.30, 2.75, and 2.45. NACA RM L8H13, 1948.
2. Faget, Maxime A., Watson, Raymond S., and Bartlett, Walter A., Jr.: Free-Jet Tests of a 6.5-Inch-Diameter Ram-Jet Engine at Mach Numbers of 1.81 and 2.00. NACA RM L50L06, 1951.
3. Staff of the Computing Section, Center of Analysis (Under Direction of Zdeněk Kopal): Tables of Supersonic Flow Around Cones. Tech. Rep. No. 1, M.I.T., 1947.
4. Luidens, Roger W., and Hunczak, Henry: Preliminary Investigation of Cone-Type Diffusers Designed for Minimum Spillage at Inlet. NACA RM E7K19, 1948.

CONFIDENTIAL

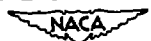
TABLE I.- TEST REYNOLDS NUMBER

Free-jet Mach number	Reynolds number (based upon inlet diameter)
1.62	5.05×10^6 to 5.71×10^6
2.00	6.46 to 6.90
2.53	6.78 to 7.62
3.05	6.28 to 7.26

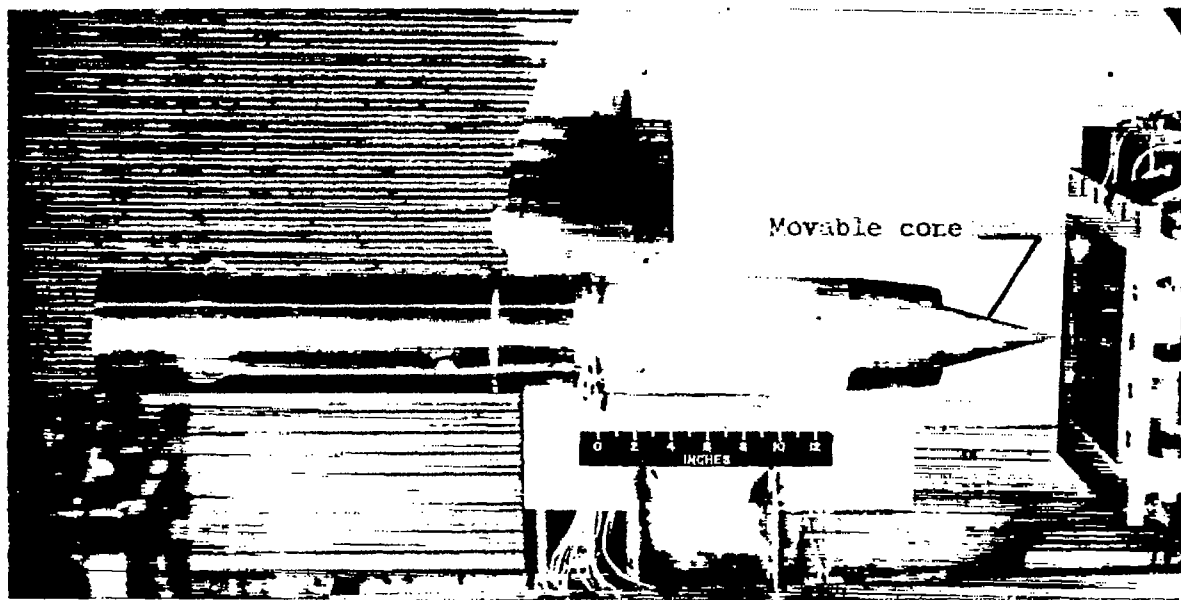


TABLE II.- COORDINATES FOR 15° SEMIANGLE MOVABLE-CONE
VARIABLE-GEOMETRY RAM-JET INLET MODEL

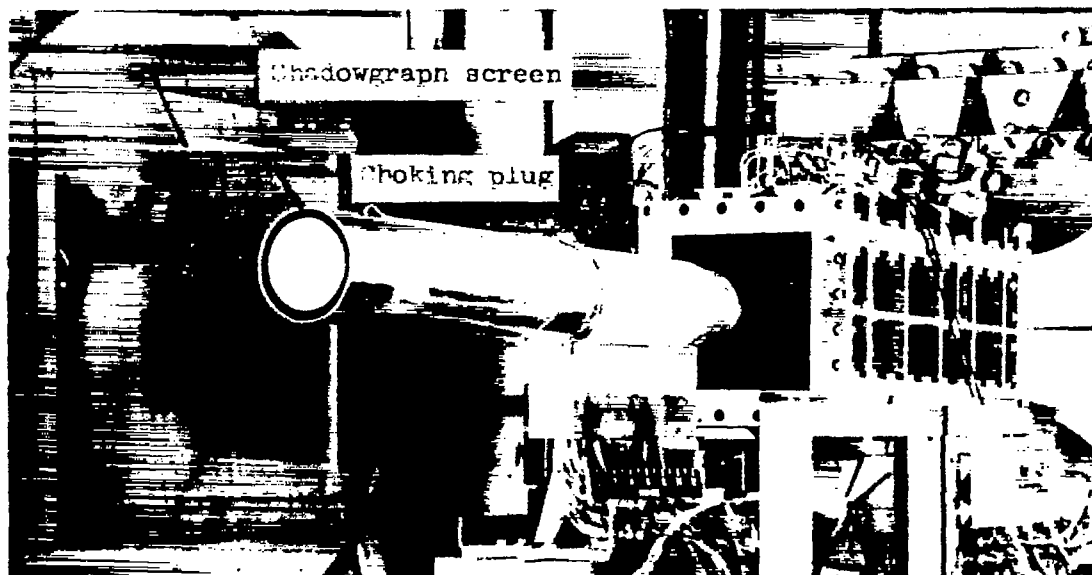
Diffuser-cowl coordinates			Movable-cone coordinates	
Station	Radius (in.)		Station (a)	Radius (in.)
	External	Internal		
0	2.745	2.740	0	0
.250	2.803	2.766	7.950	2.129
.500	2.850		8.200	2.189
.750	2.898		8.450	2.220
1.000	2.932	Straight line	8.700	2.230
			8.950	2.220
			9.200	2.202
			11.200	2.031
2.000		2.949		
2.250	Straight line	2.973		
2.500		2.987		
2.750		2.995		
3.000		3.000		
4.000	3.250	Straight line		
4.250	3.274			
4.500	3.290			
4.750	3.298			
5.000	3.300			
5.250	3.300	3.000		



^aStraight line between station 0 to 7.950 and
station 9.200 to 11.200.



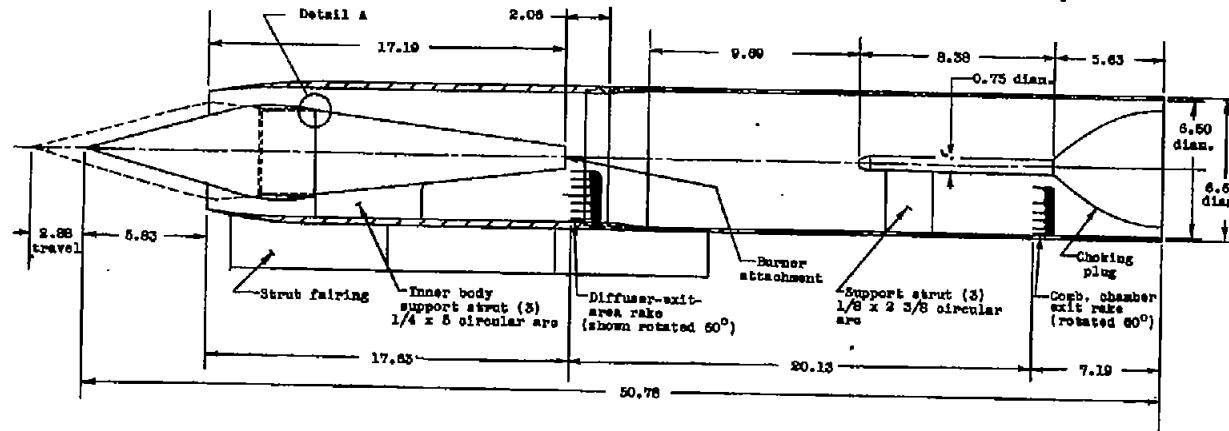
(a) Side view.



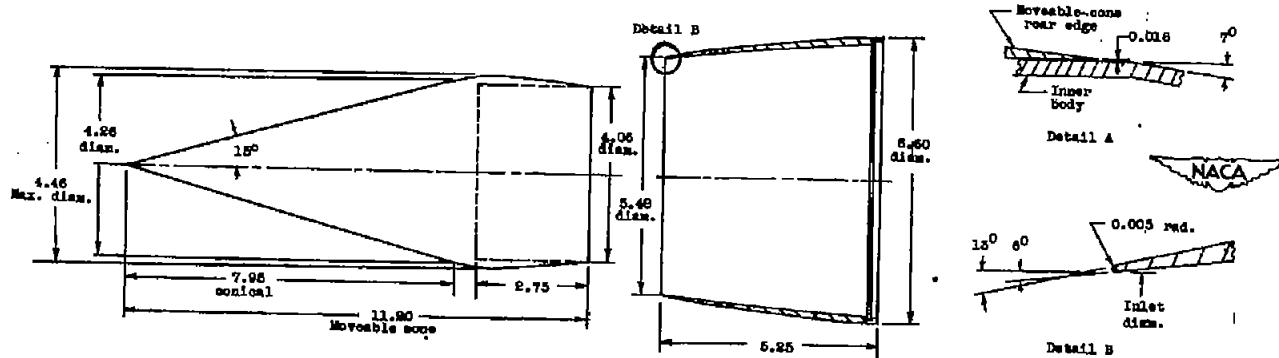
(b) Three-quarter rear view.

NACA
L-77022

Figure 1.- The ram-jet inlet model in test position in the 12- by 12-inch nozzle.



(a) Ram-jet diffuser model.



(b) Details of inlet.

Figure 2.- Schematic diagram of movable-cone variable-geometry ram-jet inlet showing principal dimensions of the model and details of the inlet. All dimensions are in inches.

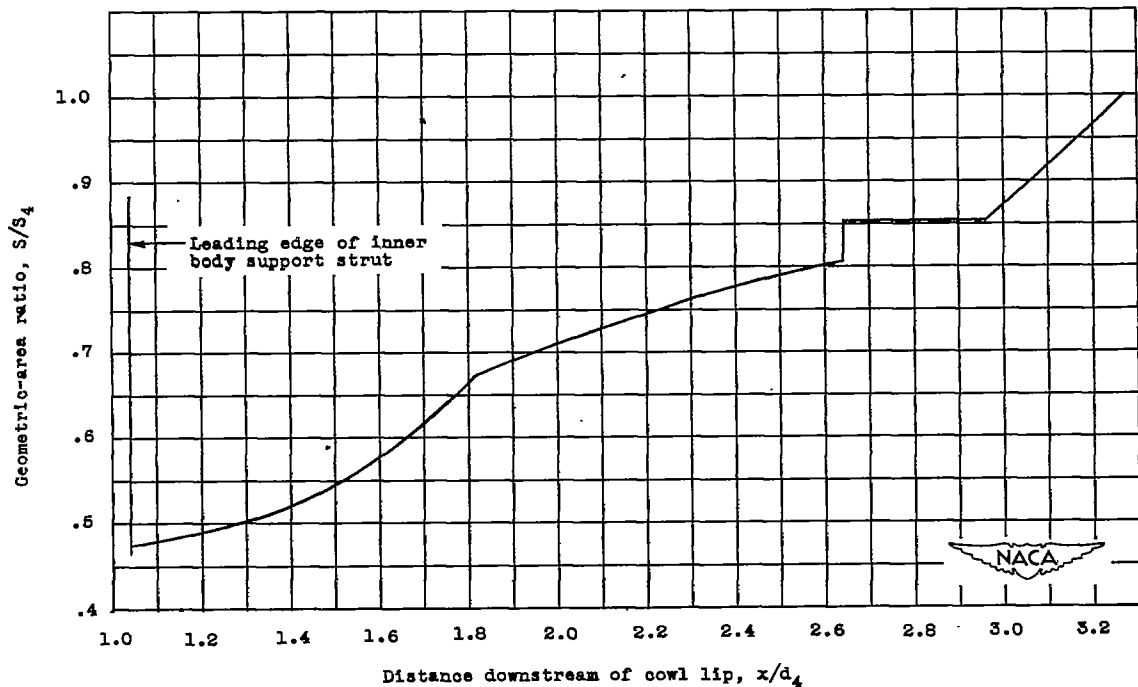


Figure 3.- Longitudinal variation of geometric-area ratio.

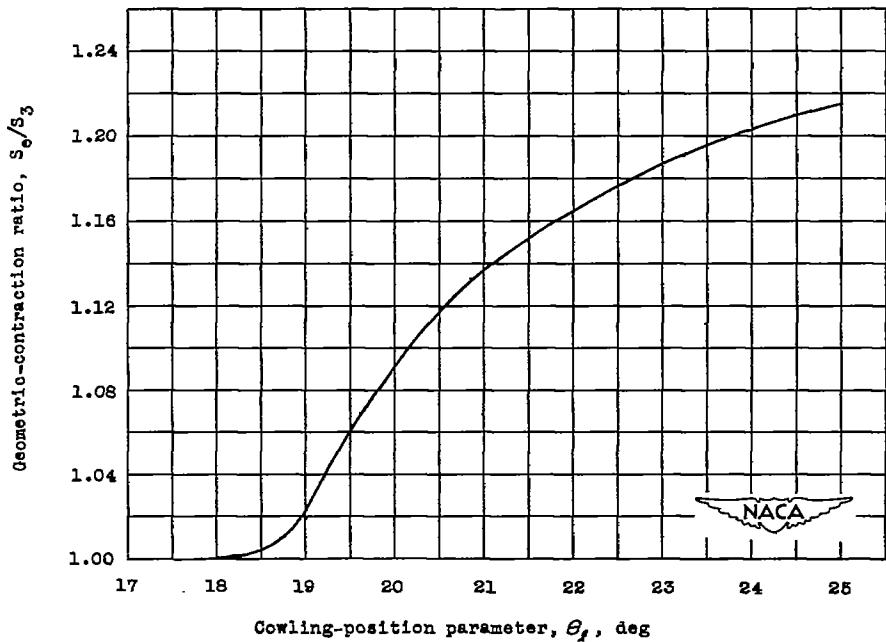


Figure 4.- Geometric-contraction ratio as a function of the cowling-position parameter.

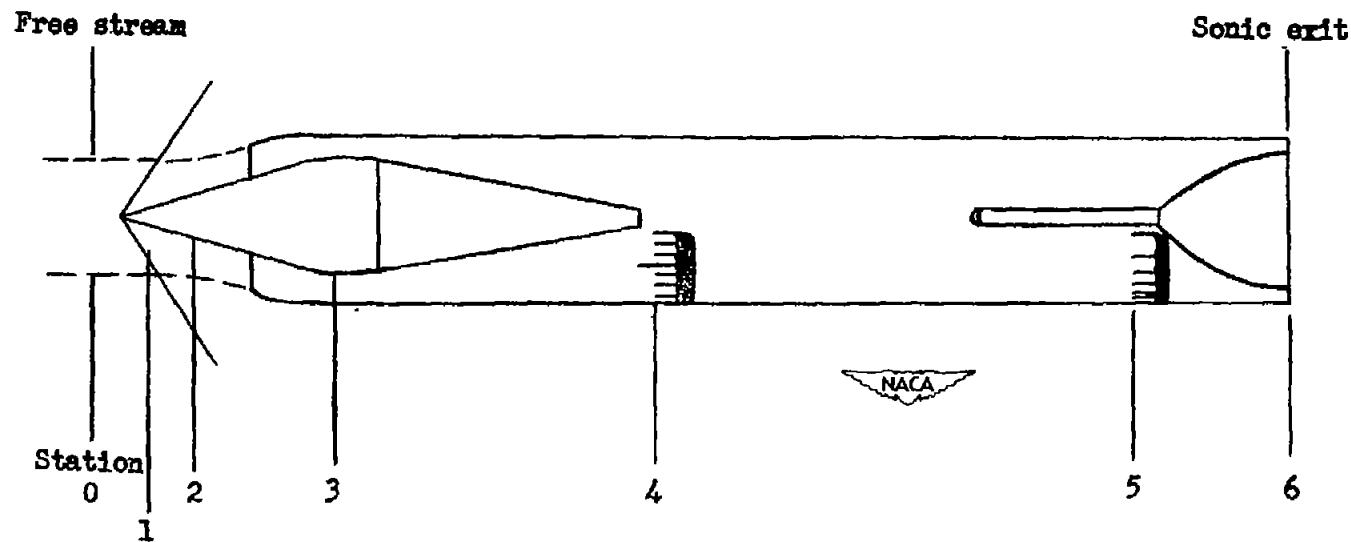


Figure 5.- Station notation for ram-jet inlet model.

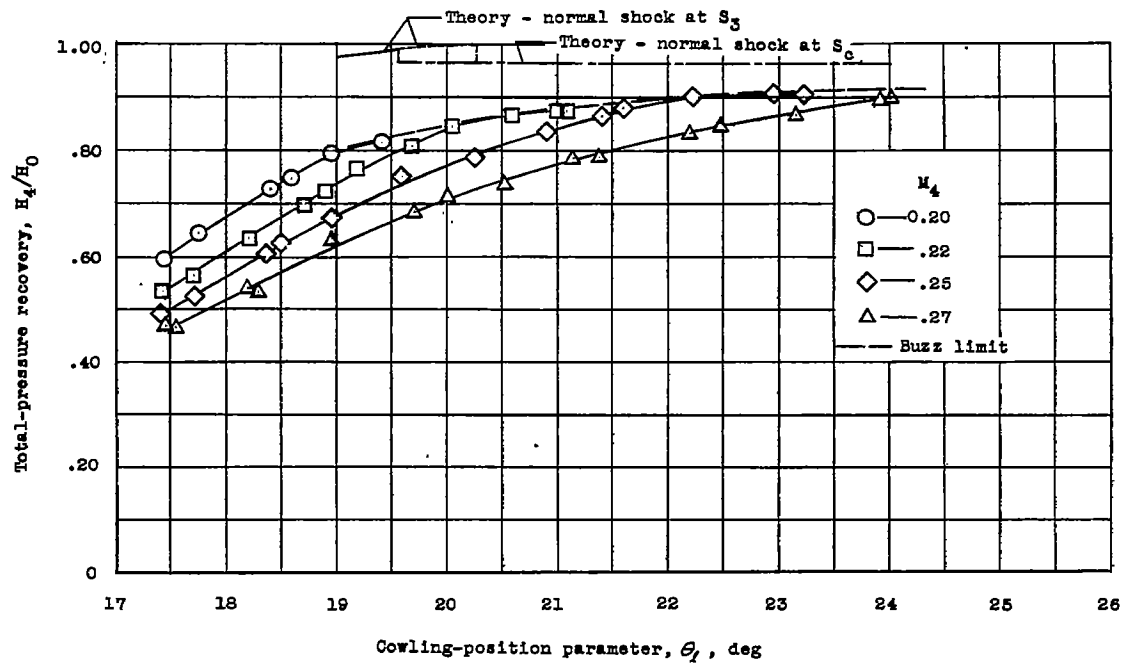
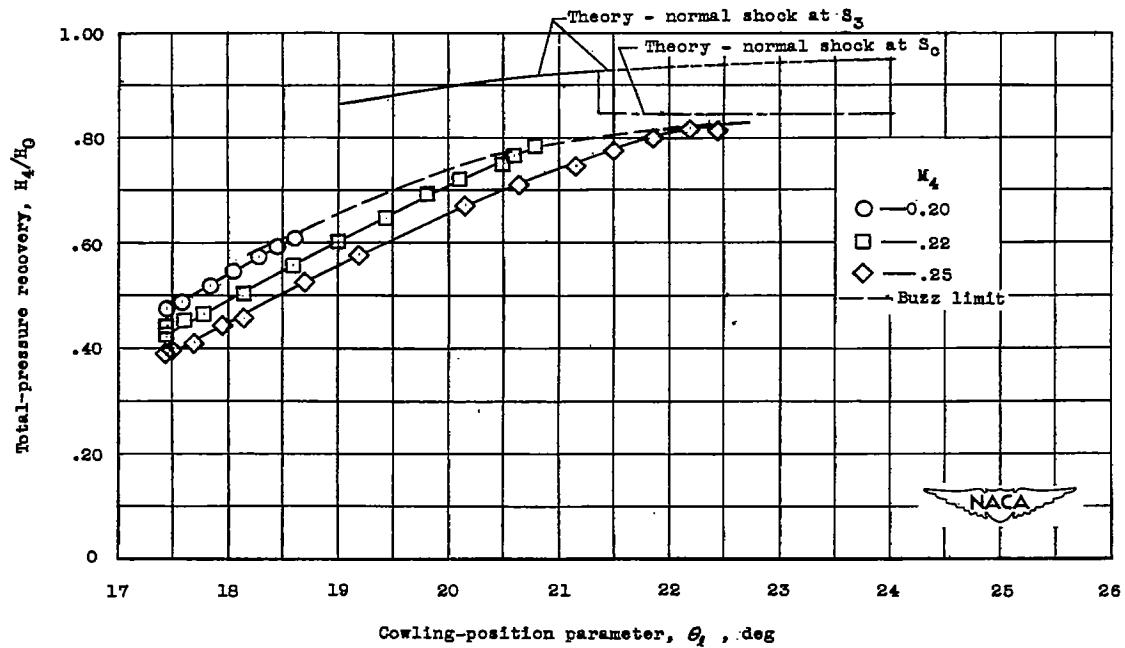
(a) $M_0 = 1.62$.(b) $M_0 = 2.00$.

Figure 6.- Total-pressure recovery as a function of the cowling-position parameter.

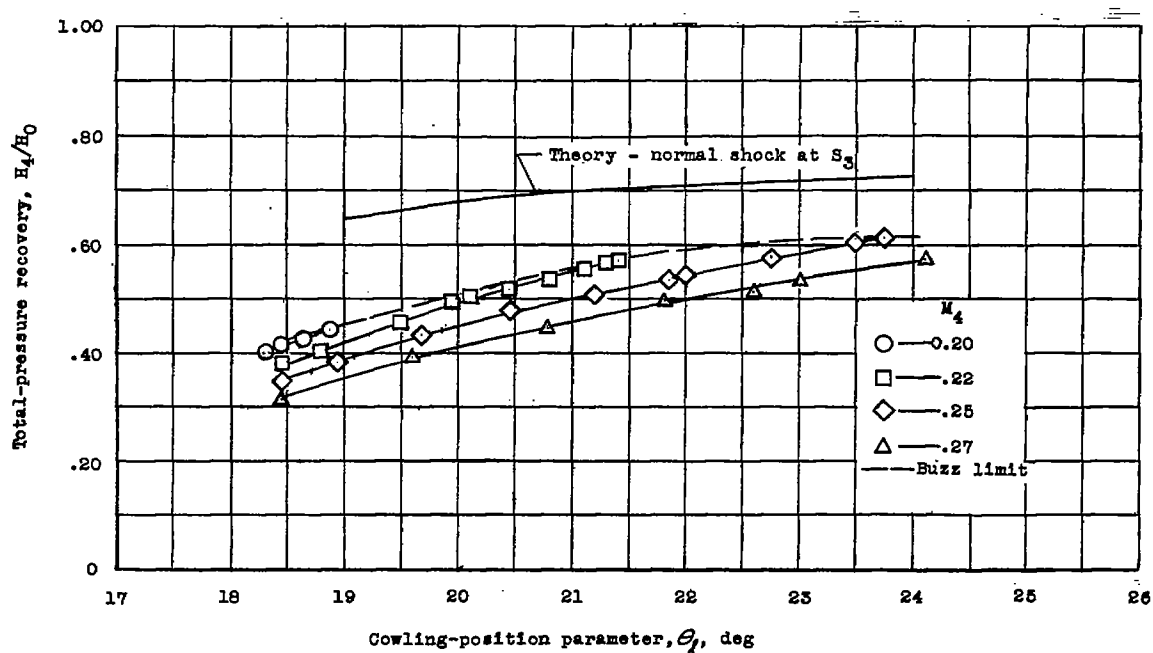
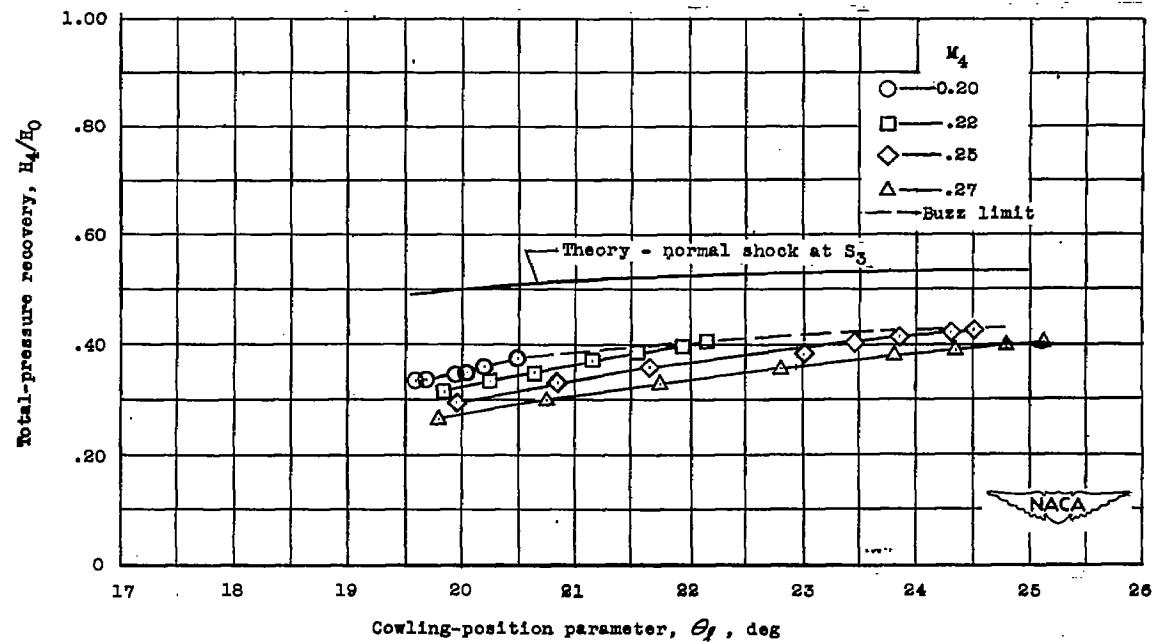
(c) $M_0 = 2.53.$ (d) $M_0 = 3.05.$

Figure 6.- Concluded.

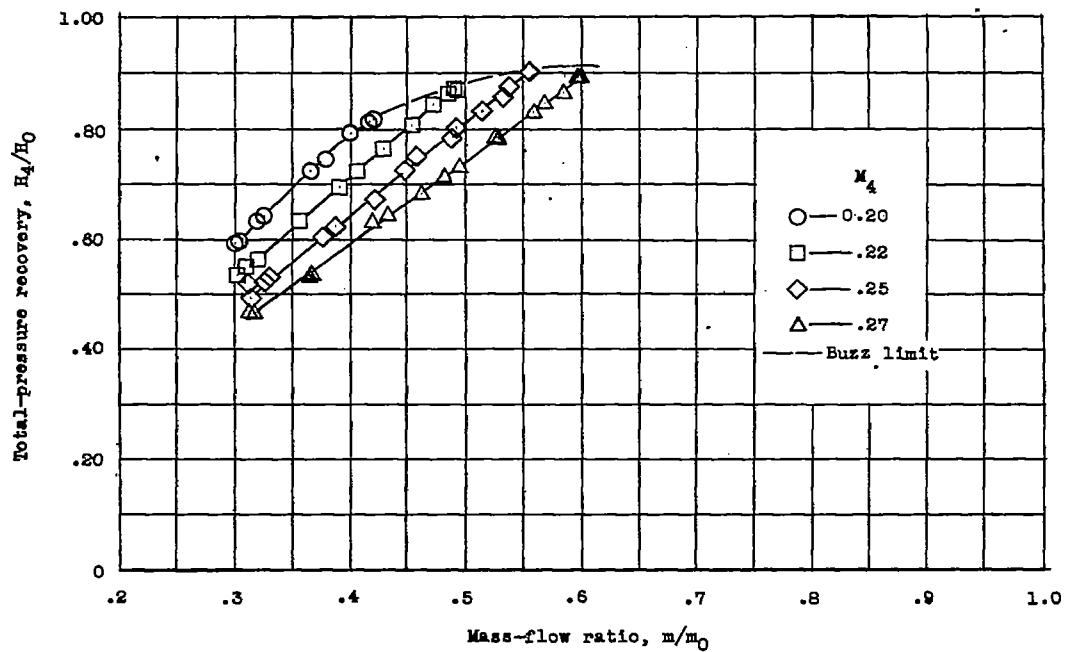
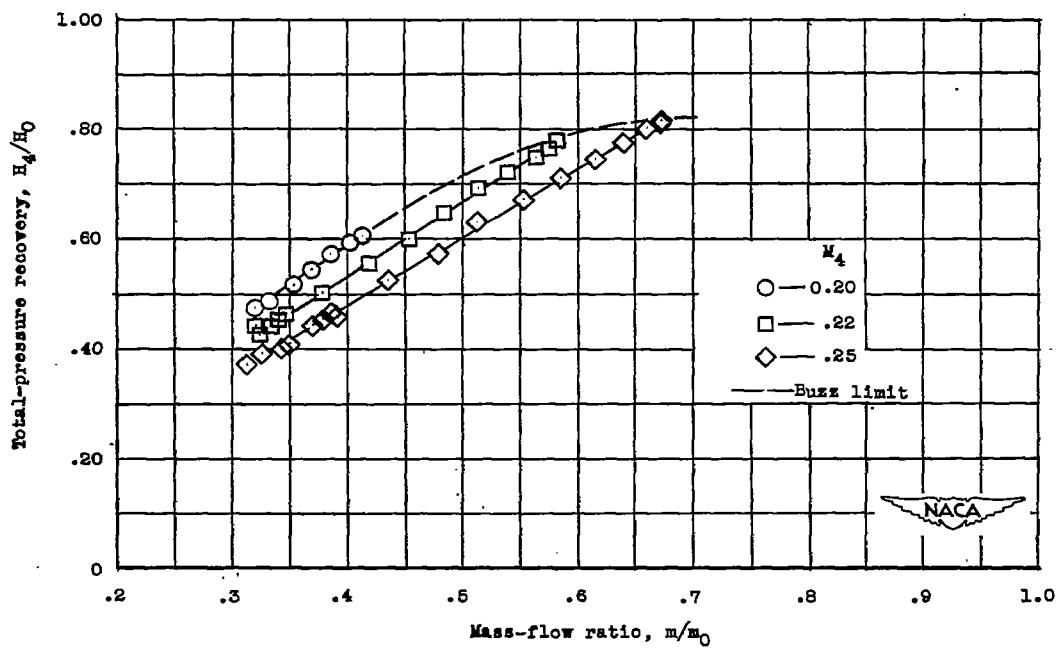
(a) $M_0 = 1.62$.(b) $M_0 = 2.00$.

Figure 7.- Total-pressure recovery as a function of the mass-flow ratio.
Cowling-position parameter varies.

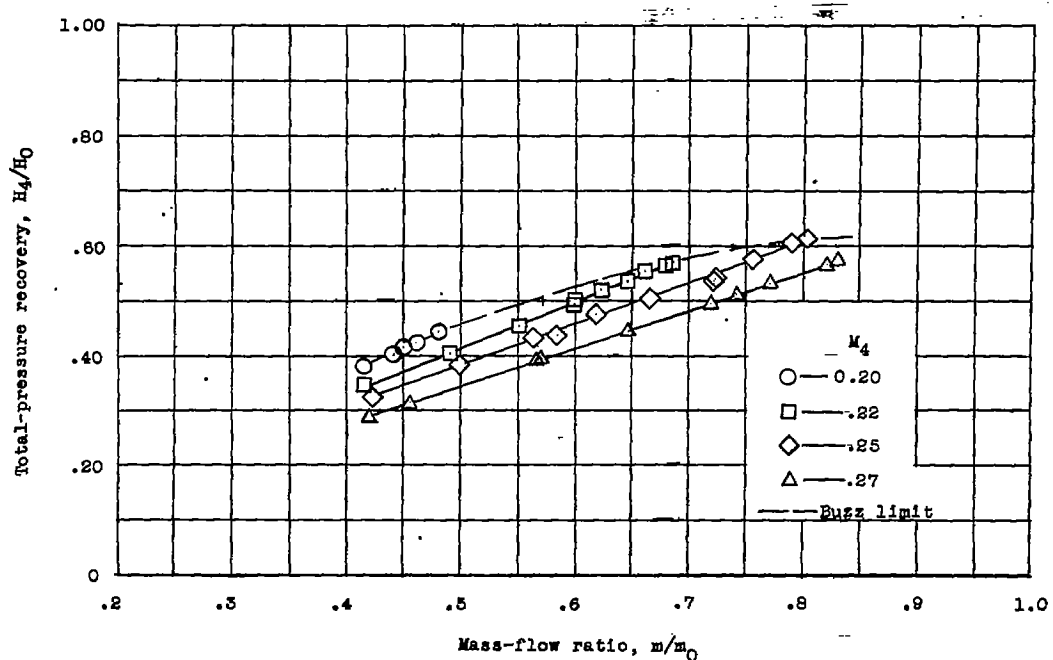
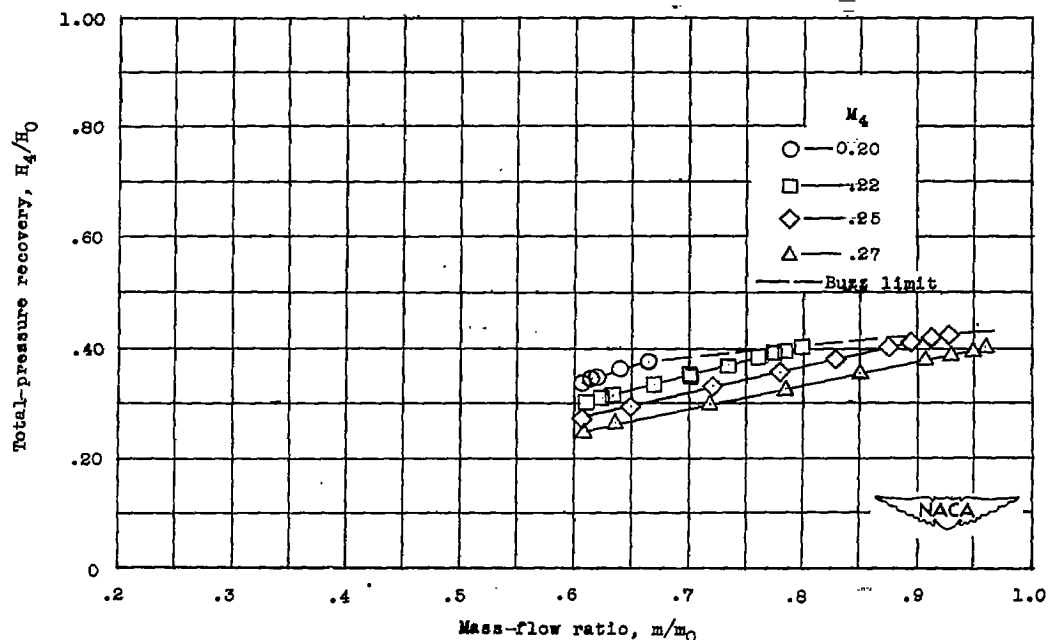
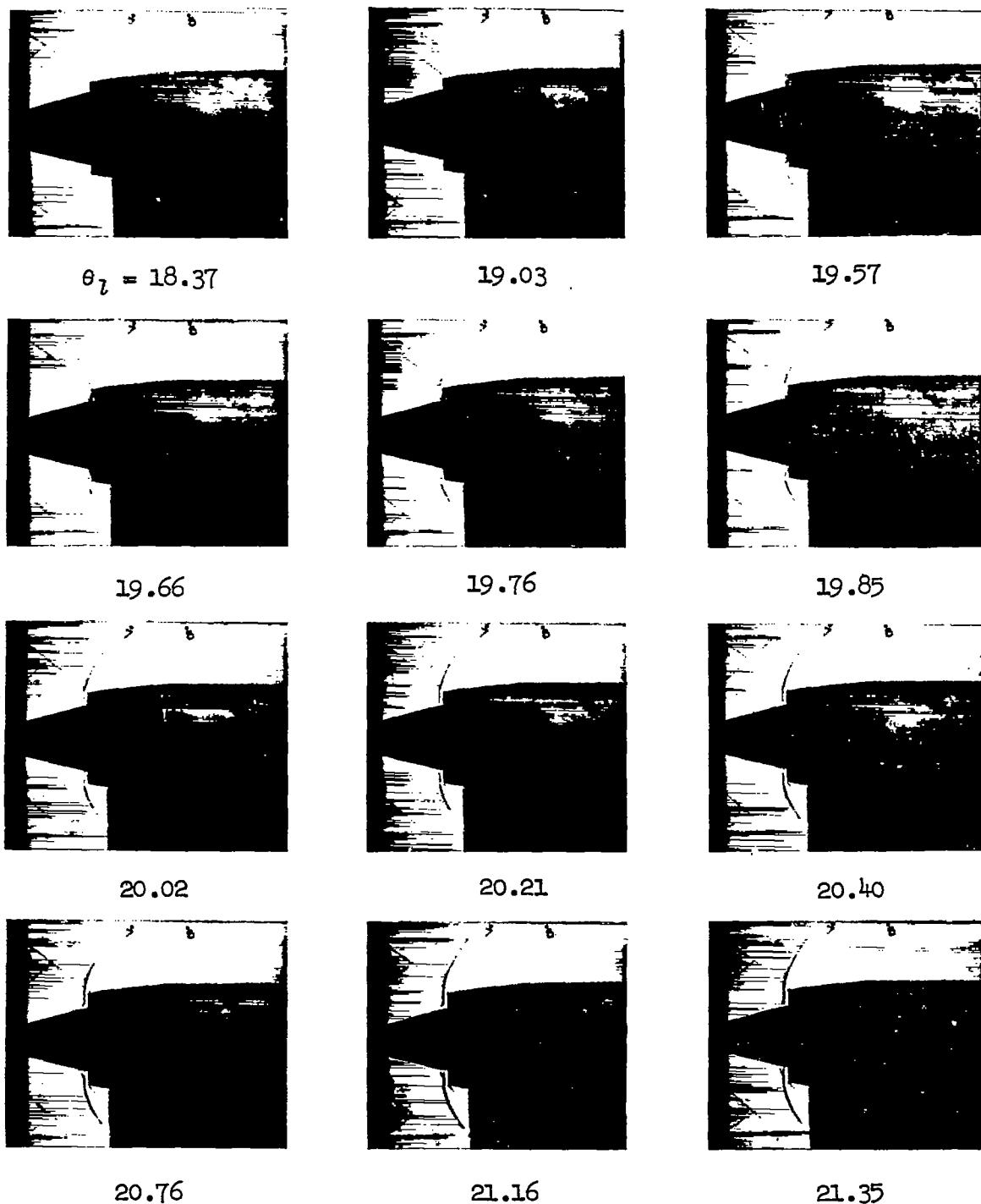
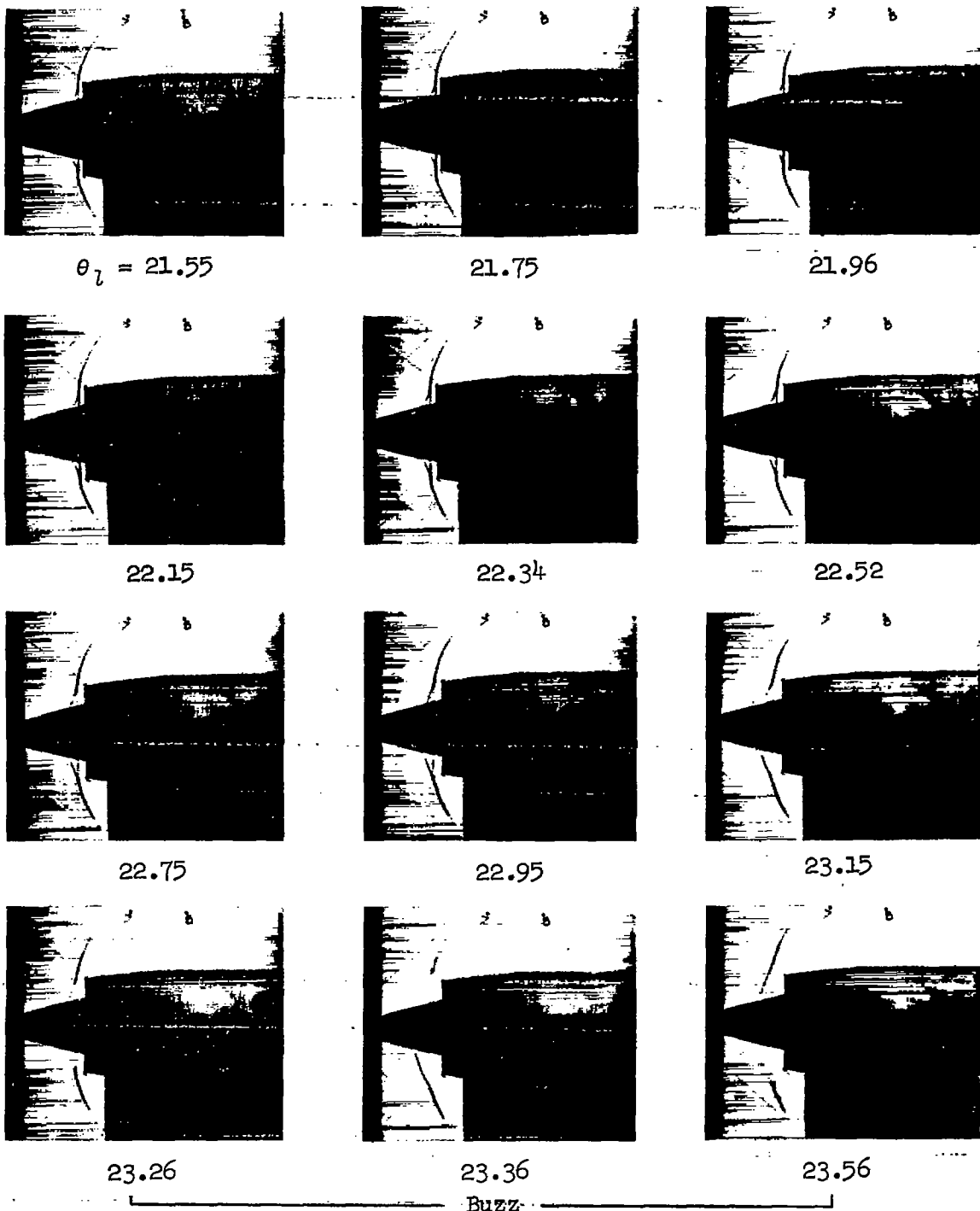
(c) $M_0 = 2.53$.(d) $M_0 = 3.05$.

Figure 7. - Concluded.

(a) $M_0 = 1.62$; $M_4 = 0.25$.

NACA
L-77023

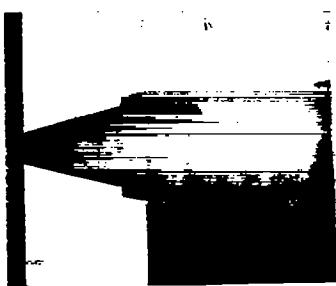
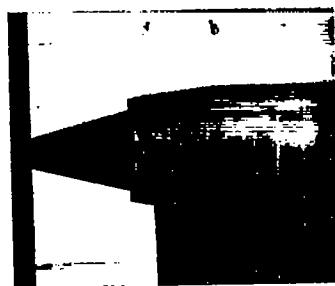
Figure 8.- Typical flow patterns for the movable-cone ram-jet inlet model for a range of free-jet Mach numbers. 15° semiangle cone; 0° angle of attack.



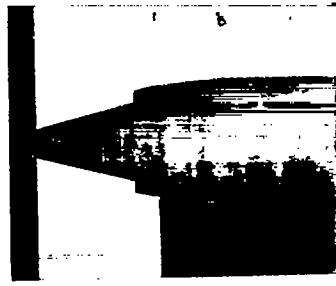
(a) Concluded.


L-77024

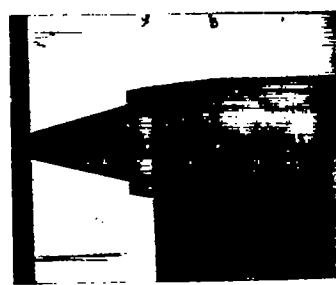
Figure 8.- Continued.

 $\theta_l = 18.15$ 

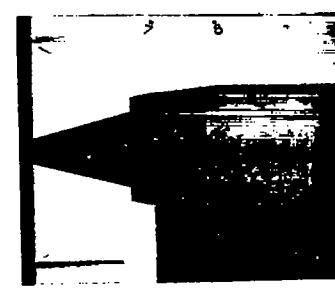
18.72



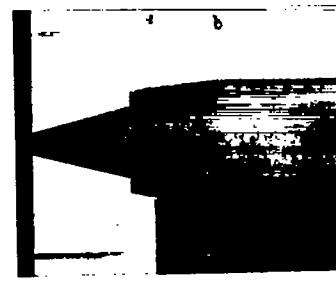
19.24



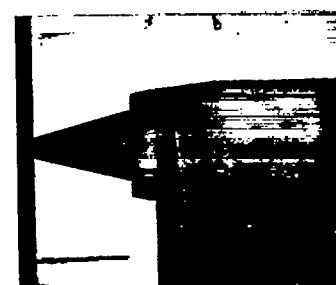
19.73



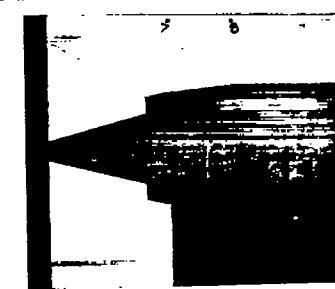
20.20



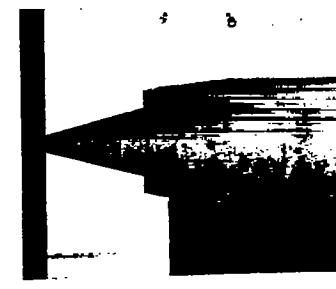
20.65



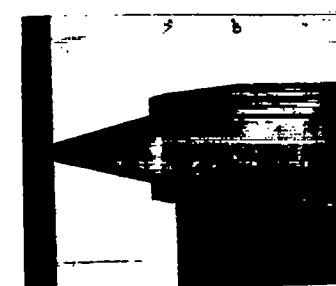
21.08



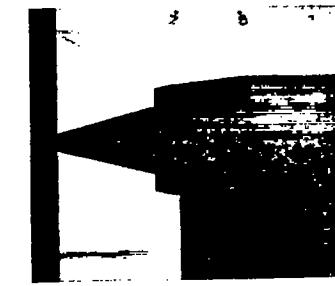
21.55



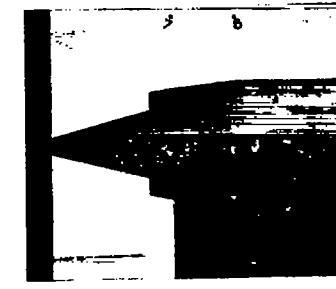
21.93



22.02



22.11



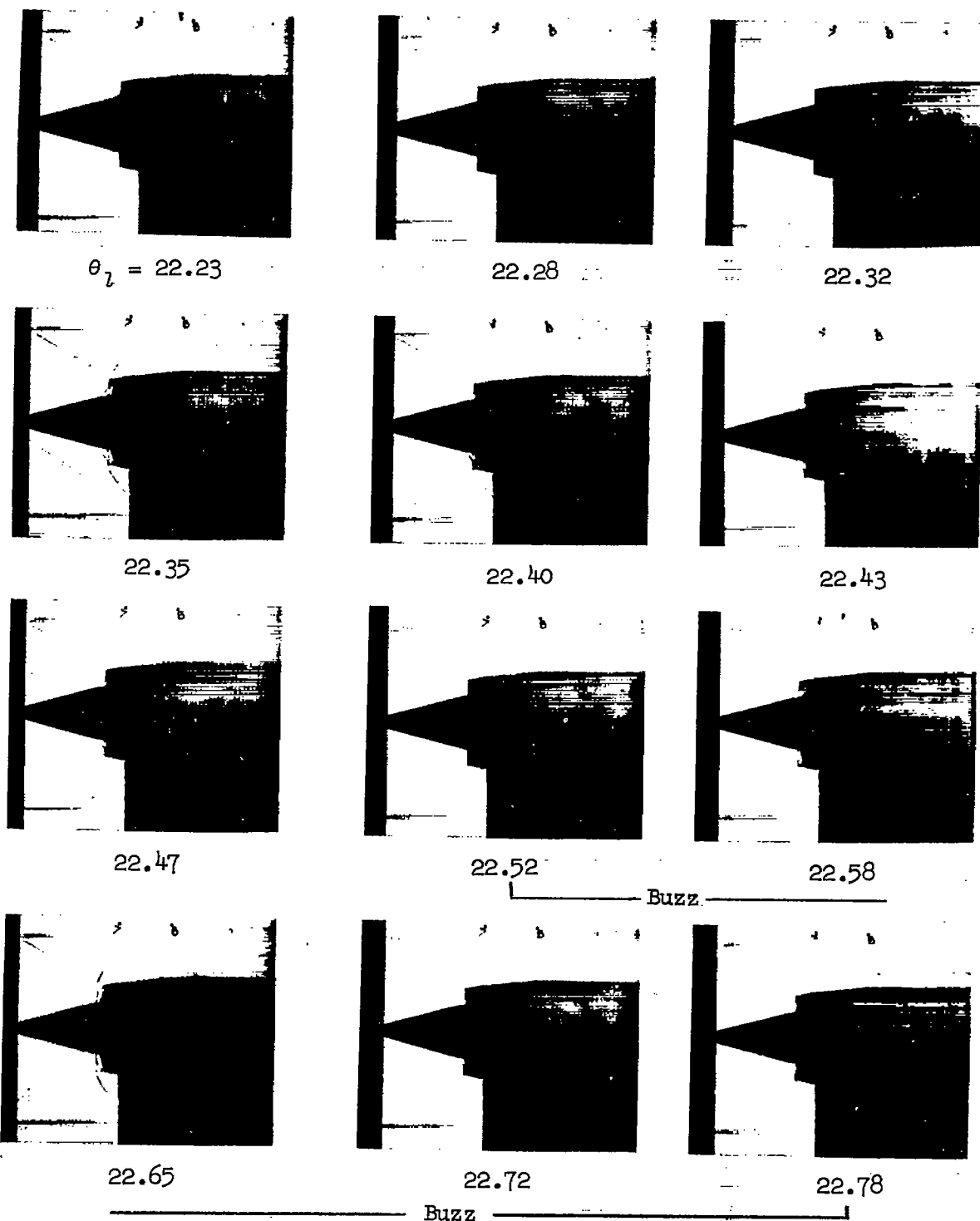
22.20

(b) $M_0 = 2.00$; $M_{\infty} = 0.25$.

Figure 8.- Continued.



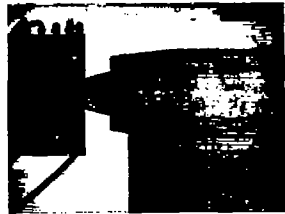
L-77025



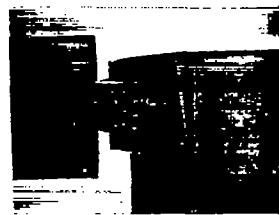
(b) Concluded.



Figure 8.- Continued. L-77026

~~CONFIDENTIAL~~ $\theta_l = 19.42$ $M_{l4} = 0.27$ 

24.10

 $\theta_l = 19.60$ $M_{l4} = 0.20$
Buzz(c) $M_0 = 2.53.$  $\theta_l = 23.11$ 

24.60

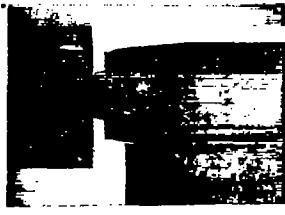
24.46
Buzz(d) $M_0 = 3.05; M_{l4} = 0.25.$

Figure 8.- Concluded.

L-77027

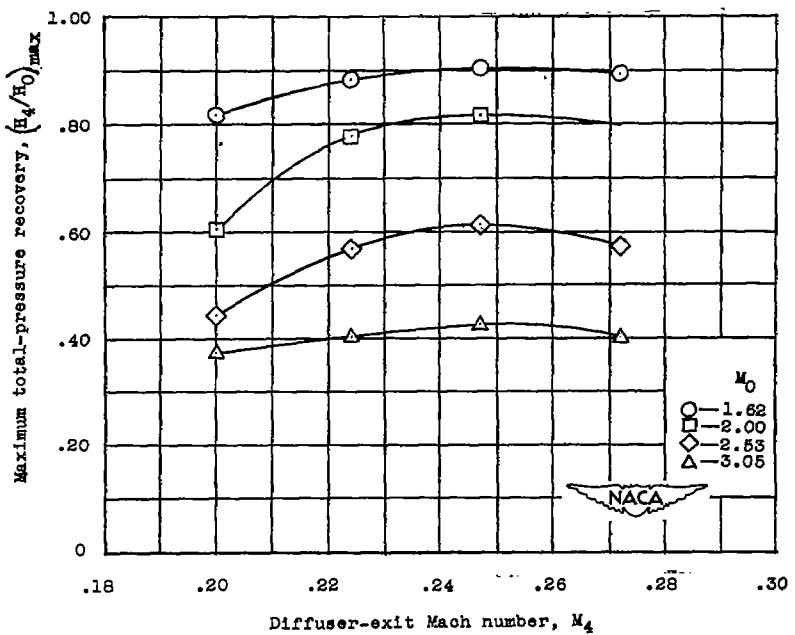


Figure 9.- Maximum total-pressure recovery obtained as a function of diffuser-exit Mach number.

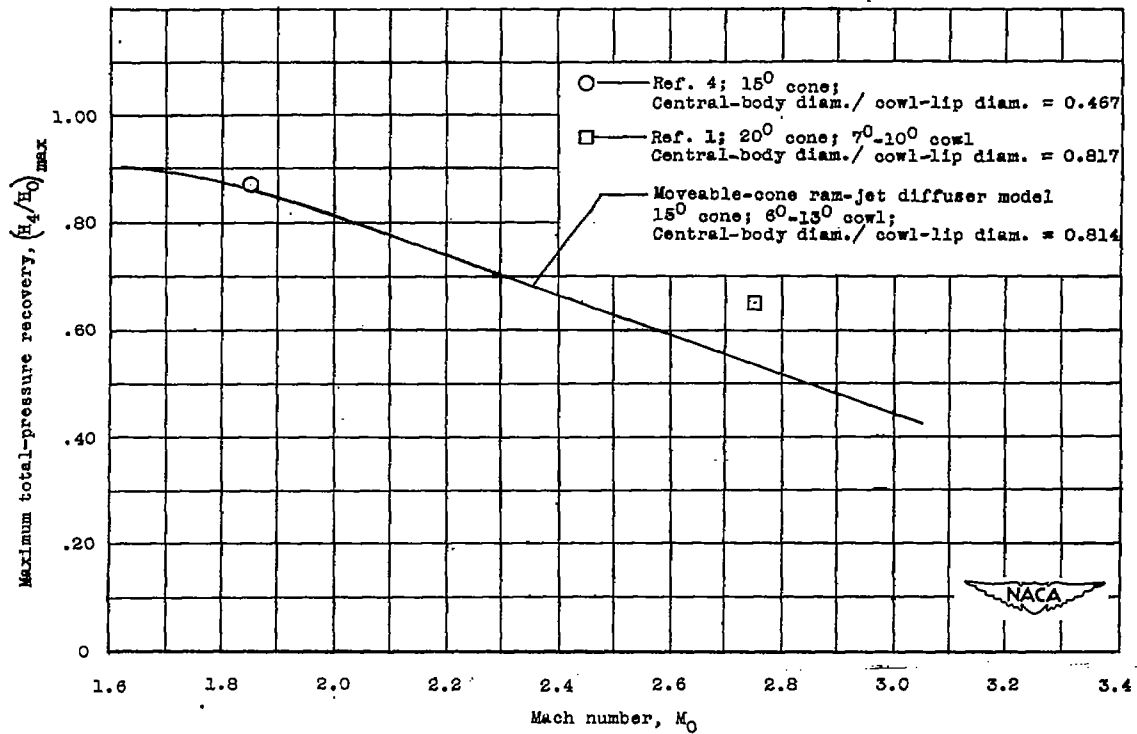


Figure 10.- Maximum total-pressure recovery variation with Mach number.

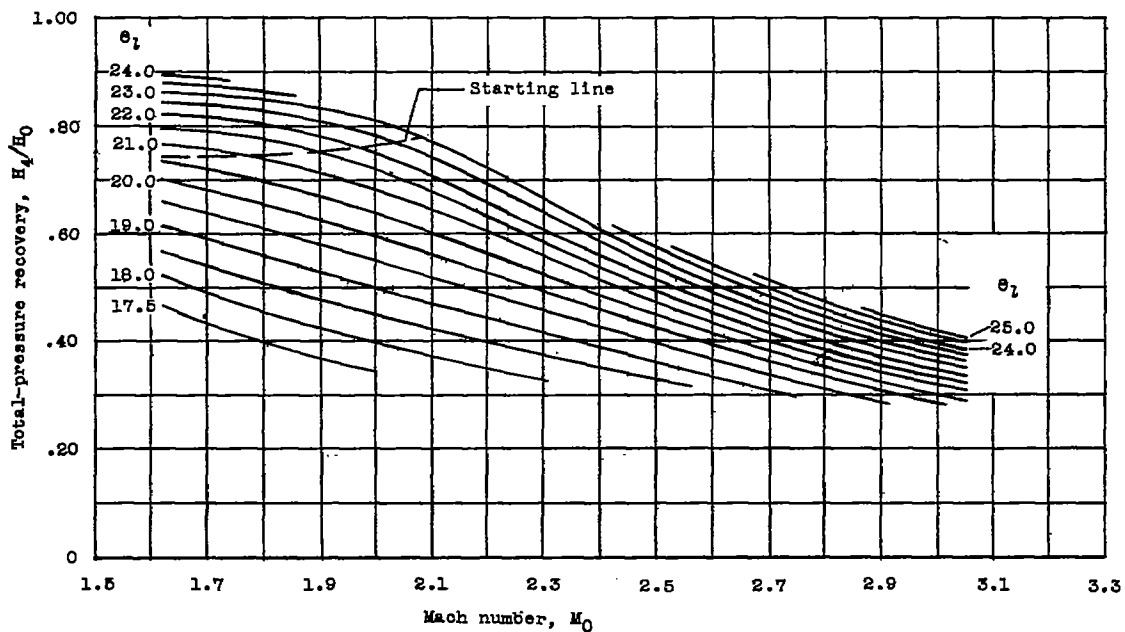
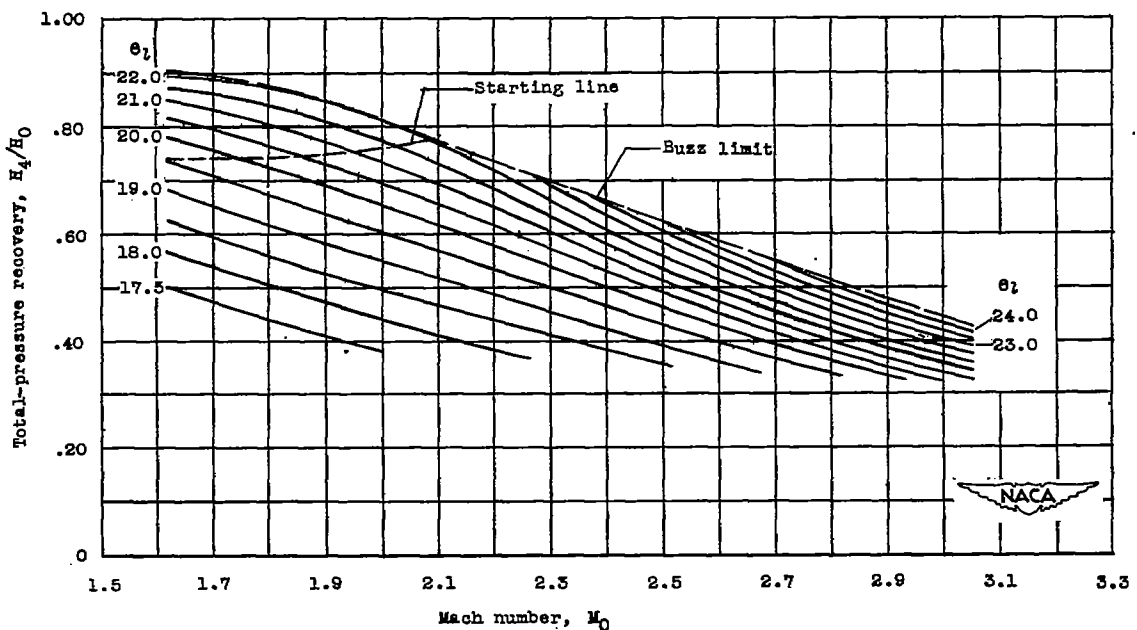
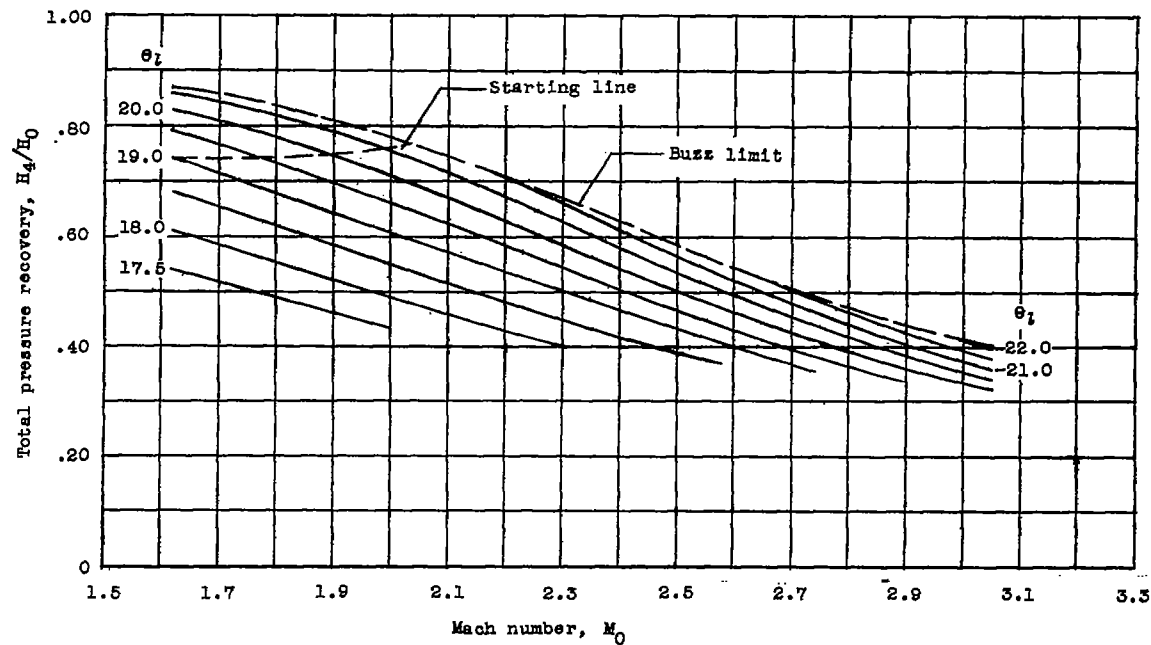
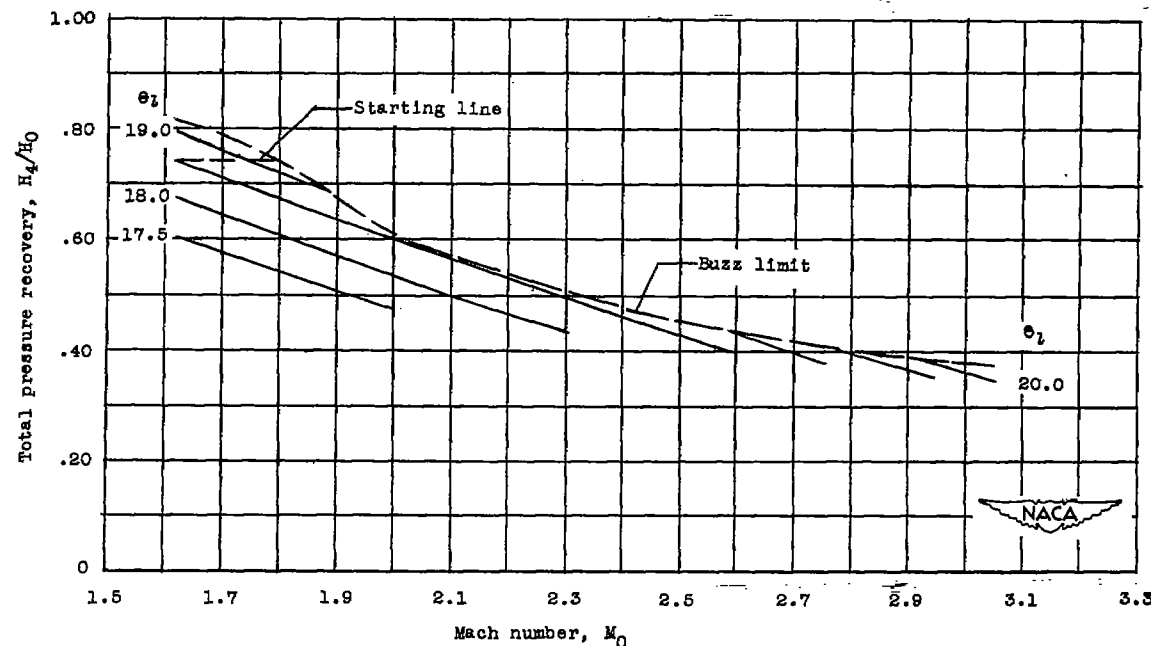
(a) $M_4 = 0.27$.(b) $M_4 = 0.25$.

Figure 11.- Total-pressure recovery as a function of free-jet Mach number with lines of constant cowling-position parameter θ_l .



(c) $M_4 = 0.22.$



(d) $M_4 = 0.20.$

Figure 11.- Concluded.

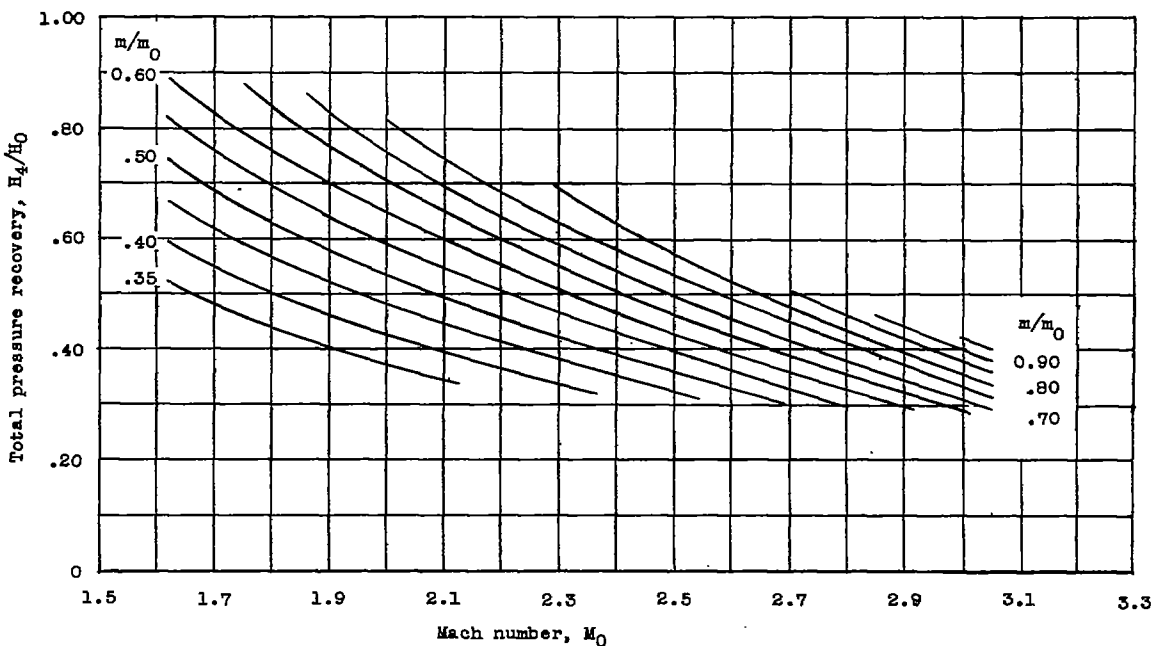
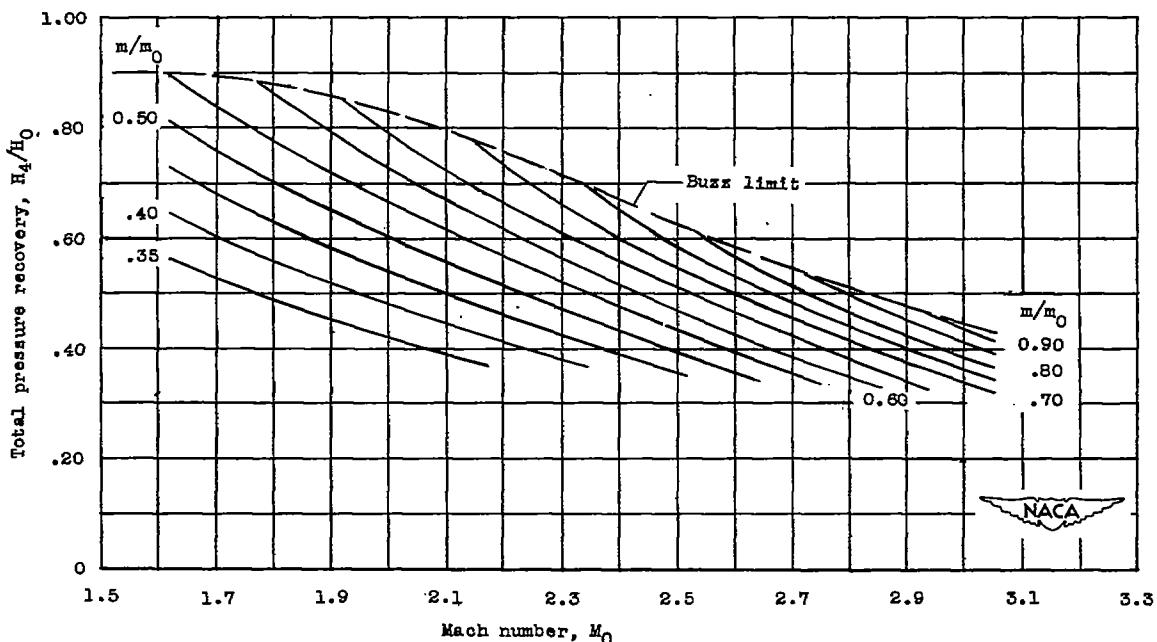
(a) $M_4 = 0.27$.(b) $M_4 = 0.25$.

Figure 12.- Total-pressure recovery as a function of free-jet Mach number with lines of constant mass-flow ratio.

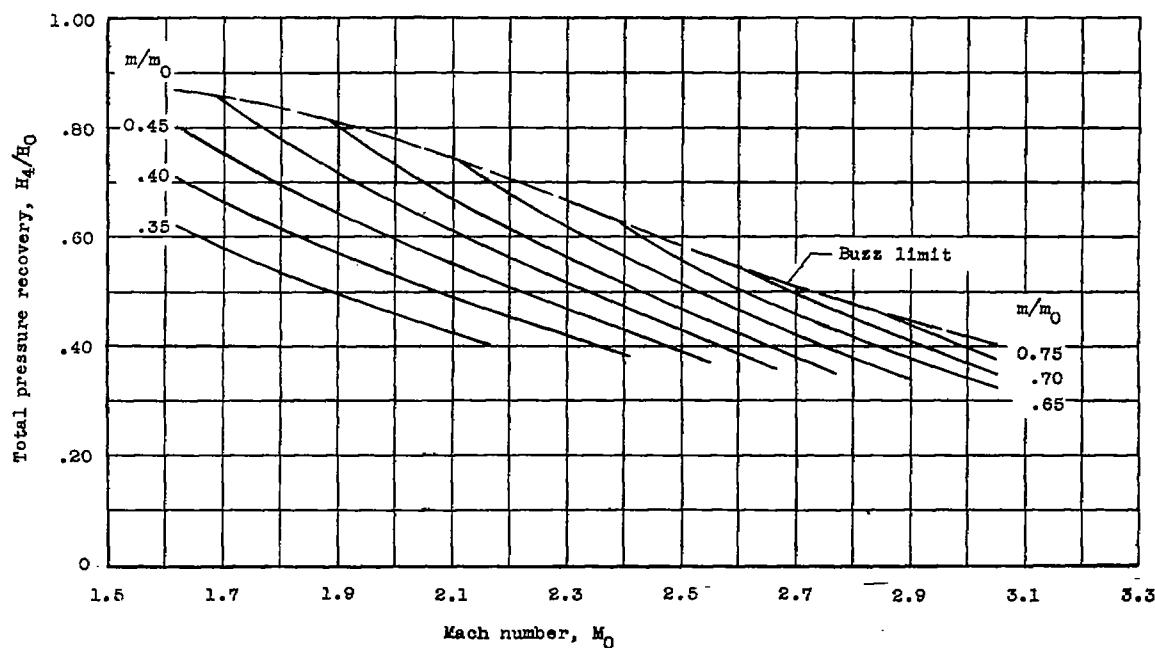
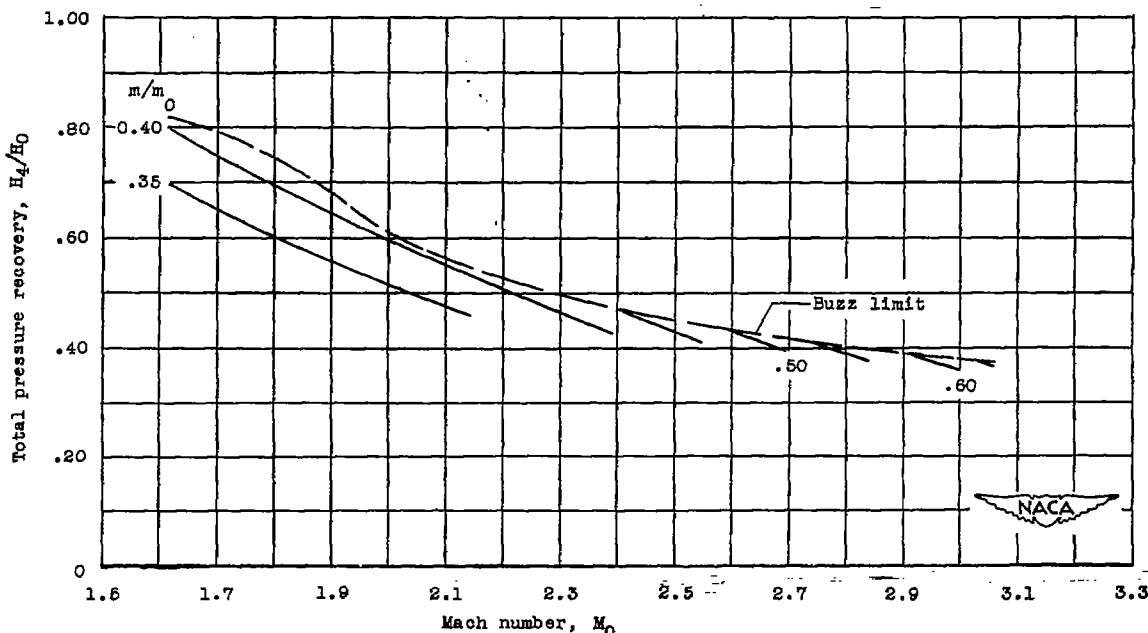
(c) $M_4 = 0.22$.(d) $M_4 = 0.20$.

Figure 12.- Concluded.